

# Defect cluster formation and radiation hardening in molybdenum neutron-irradiated at 80 °C

Meimei Li <sup>a,\*</sup>, N. Hashimoto <sup>a,b</sup>, T.S. Byun <sup>a</sup>, L.L. Snead <sup>a</sup>, S.J. Zinkle <sup>a</sup>

<sup>a</sup> *Materials Science and Technology Division, Oak Ridge National Laboratory, P.O. Box 2008, MS 6138, Oak Ridge, TN 37831, United States*

<sup>b</sup> *Now at: Materials Science Division, Hokkaido University, Sapporo 060-8628, Japan*

## Abstract

Molybdenum was neutron-irradiated near 80 °C to doses of  $7.2 \times 10^{-5}$ ,  $7.2 \times 10^{-4}$ ,  $7.2 \times 10^{-3}$ , 0.072 and 0.28 dpa. Post-irradiation examination included electrical resistivity and tensile properties measured at room temperature. Microstructure of irradiated specimens was examined by TEM and the defect cluster density and cluster mean size were characterized. Measurements of electrical resistivity and cluster density showed sublinear defect accumulation behavior. The mean size of visible defect clusters increased with increasing dose. Yield stress decreased at  $7.2 \times 10^{-5}$  and  $7.2 \times 10^{-4}$  dpa, then increased significantly with increasing dose up to 0.072 dpa and saturated. It appeared that there was a transition in hardening from weak obstacles to strong obstacles. It is suggested that the formation of sessile defect clusters in neutron-irradiated Mo is mainly associated with diffusive nucleation and growth rather than in-cascade clustering.

Published by Elsevier B.V.

## 1. Introduction

Molybdenum is of interest for many nuclear reactor applications due to its high melting point, excellent high temperature strength, good thermal conductivity and resistance to irradiation swelling. Whether or not the inferior resistance to radiation embrittlement can be improved depends largely on the formation process of sessile defect clusters. If the cluster formation is associated with nucleation and growth processes, solute additions or defect sinks associated with precipitates may have a strong effect on radiation hardening and embrittlement

behavior. Conversely, alloying would have a relatively weak effect if clusters originate from displacement cascades. In general, in-cascade formation of sessile defect clusters is enhanced with increasing atomic weight due to increasing compactness of displacement cascades. Both experimental studies and molecular dynamics computer simulations have provided strong evidence for in-cascade defect cluster formation in the face-centered cubic (fcc) metals Ni, Cu, Ag, Pt and Au and the bcc metal W; in-cascade defect cluster formation was not observed in the fcc metal Al and the bcc metals Fe and V [1–3]. There are insufficient experimental data to determine the cluster formation process in neutron-irradiated Mo. Defect yield data in the literature on ion-irradiated Mo suggested that the nucleation and growth process may be significant in Mo [2].

\* Corresponding author. Tel.: +1 865 5761813; fax: +1 865 2413650.

E-mail address: [lim1@ornl.gov](mailto:lim1@ornl.gov) (M. Li).

This study investigated defect cluster formation and the resultant irradiation hardening in Mo due to low temperature and low dose neutron irradiation. The experimental results are analyzed to differentiate the roles of in-cascade clustering and diffusive nucleation and growth.

## 2. Experimental procedure

The material examined was low carbon arc cast (LCAC) molybdenum (>99.95%). Subsize SS-3 tensile specimens had gauge dimensions of  $7.62 \times 1.52 \times 0.50$  mm; coupon specimens were  $25.4 \times 4.95 \times 0.25$  mm. Annealing at 1200 °C for 1 h in vacuum resulted in an equiaxed grain size of 70  $\mu$ m.

Irradiation in perforated capsules in the hydraulic tube facility of the High Flux Isotope Reactor in contact with the coolant maintained the specimen temperature at  $\sim 80$  °C. Irradiation to fluences in the range of  $2 \times 10^{21}$  to  $8 \times 10^{24}$  n/m<sup>2</sup> ( $E > 0.1$  MeV) corresponds to displacement damage levels of  $7.2 \times 10^{-5}$  to 0.28 dpa. Unexpected weight loss and thickness reduction was observed in specimens irradiated to high neutron fluences due to corrosion of molybdenum in flowing water. After ultrasonically cleaning in ethanol, only discontinuous areas of discoloration remained.

Electrical resistivity of SS-3 tensile specimens was measured at room temperature before and after irradiation using a four-point probe technique. Tensile tests were conducted on unirradiated and irradiated specimens at room temperature at a strain rate of  $1 \times 10^{-3}$  s<sup>-1</sup>. The irradiated microstructure was examined in a JEOL JEM-2000FX transmission electron microscope (TEM) operating at 200 kV. The 3 mm TEM discs were electropolished in a Tenupol twin-jet polishing unit. TEM examination used combined bright field (BF) and weak beam dark field (WBDF) imaging. Weak beam dark field imaging conditions were ( $g/6g$ ,  $g = 110$ ) near zone axis of  $[\bar{1}11]$ . Both defect cluster density and size measurements were made from WBDF images. The defect density measurements were checked by plotting the areal density vs. foil thickness, and the volumetric density was determined by the slope [3].

## 3. Results

### 3.1. Changes in electrical resistivity after irradiation

The dose dependence of room-temperature electrical resistivity for LCAC Mo is shown in Fig. 1.

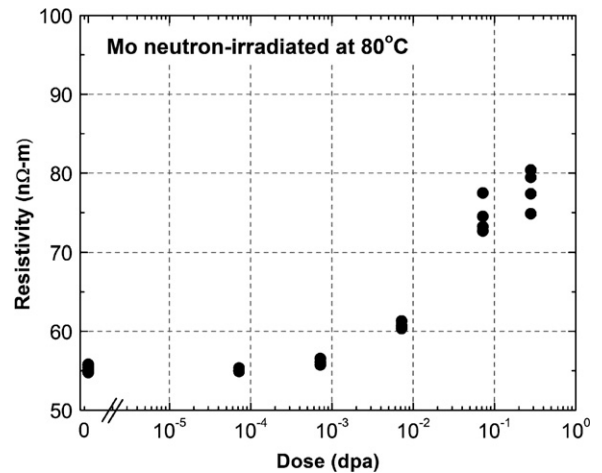


Fig. 1. Dose dependence of room-temperature electrical resistivity of neutron-irradiated LCAC Mo.

The data points for each dose are the mean values of five measurements from four unique specimens. A measurable increase in electrical resistivity was obtained at a dose 0.00072 dpa, and increased significantly with dose. The dose dependence of electrical resistivity was significantly reduced as dose increased from 0.072 dpa to 0.28 dpa. The influence of the transmutation products Tc and Ru on electrical resistivity of irradiated Mo was estimated from the literature data [4] to be about 5% of the total increase in electrical resistivity after irradiation for 267 h (0.28 dpa).

### 3.2. As-irradiated microstructure

Fig. 2 shows representative WBDF images for the LCAC Mo irradiated in the dose range  $7.2 \times 10^{-5}$  to 0.28 dpa. Two major types of defect structure were observed, defect loops and rafts. The term ‘raft’ refers to aligned groups of small dislocation loops. The nature of the small loops was not resolved. Previous studies have found that dislocation loops in neutron-irradiated Mo are predominantly interstitial-type with the Burgers vectors  $\mathbf{b} = a/2(111)$  [5–10]. Loops in rafts have the same Burgers vectors lying on the  $\{111\}$  habit planes.

The irradiated defect microstructure was characterized by cluster density, cluster mean size and size distribution. The density and mean size are plotted as a function of dose in Fig. 3, and the size distribution will be presented in future publications. Fig. 3 also includes published data on molybdenum neutron-irradiated at 50–100 °C [11–13]. This compari-

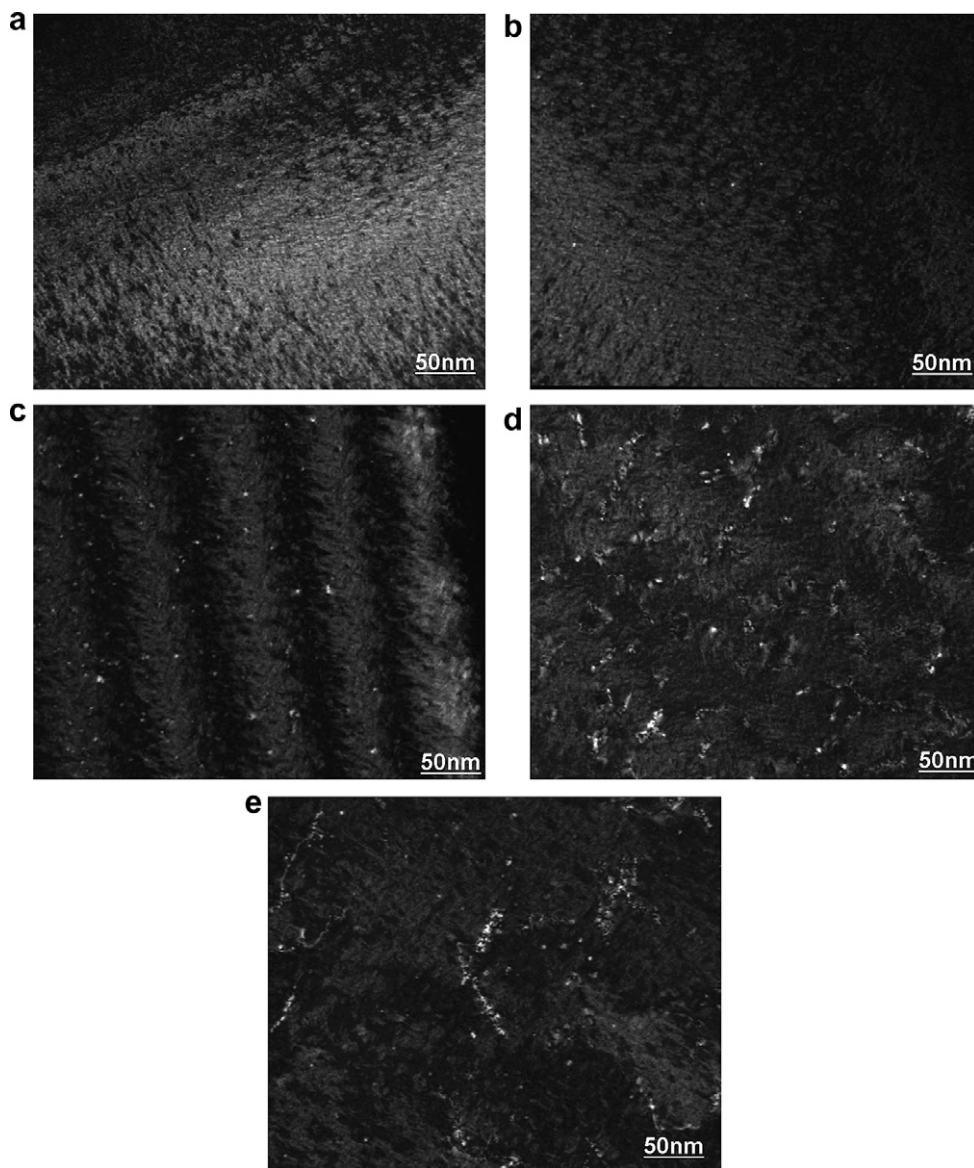


Fig. 2. Weak beam dark field images of defect clusters at different dose levels taken with a  $[\bar{1}11]$  zone axis and  $g = [110]$  ( $g/6g$ ). (a)  $7.2 \times 10^{-5}$  dpa, (b)  $7.2 \times 10^{-4}$  dpa, (c)  $7.2 \times 10^{-3}$  dpa, (d) 0.072 dpa, (e) 0.28 dpa.

son among different studies is complicated by the conversion from neutron fluence to dpa. In Fig. 3, the dpa values were cited whenever possible or a conversion of  $2.0 \times 10^{25}$  n/m<sup>2</sup>/dpa ( $E > 0.1$  MeV) or  $1.3 \times 10^{25}$  n/m<sup>2</sup>/dpa ( $E > 1$  MeV) was employed if only neutron fluences were reported. Fig. 3 shows a strong dose dependence of defect cluster density. No visible defect clusters were detected in the  $7.2 \times 10^{-5}$  dpa specimen. The cluster density increased significantly as dose increased from  $7.2 \times 10^{-4}$  to 0.0072 dpa, with clusters distributed homogeneously. In the 0.0072 dpa specimen, some defect

clusters began to form aligned groups with two or three clusters in a row, indicating onset of raft formation. The loop density increased only slightly from 0.0072 to 0.072 dpa and then decreased from 0.072 to 0.28 dpa. At high doses ( $\geq 0.072$  dpa), clusters are strongly segregated to form rafts, and the raft length increased with increasing dose. A sublinear relation between defect cluster density and dose was revealed at low and medium doses. The variation in defect cluster density between different studies is likely due to the material purity and the microscopy techniques.

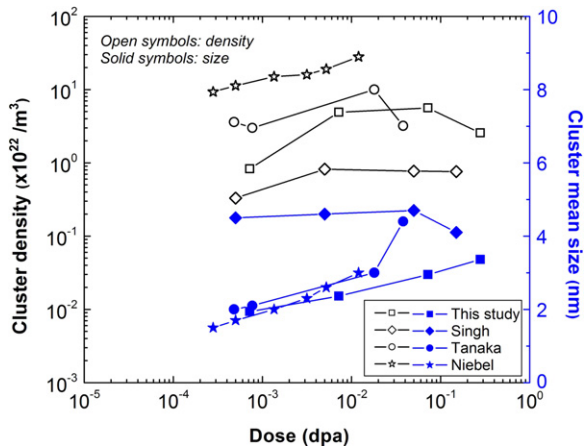


Fig. 3. Dose dependence of cluster density and mean size in Mo neutron irradiated at 50–100 °C.

The mean cluster size is dependent on irradiation dose as well, increasing with dose from 1.94 to 3.36 nm between  $7.2 \times 10^{-4}$  and 0.28 dpa with a broader size distribution at high doses. This dose dependence was also observed by Tanaka et al. [11] and Niebel and Wilkens [13]. Singh et al. [12] reported a nearly unchanged mean size of defect clusters in the mono-crystalline Mo.

### 3.3. Dose dependence of yield stress

The engineering stress–strain curves of unirradiated and irradiated Mo tested at room temperature are presented in Fig. 4. Fig. 5 shows the dose dependence of the change in lower yield stress for the LCAC Mo specimens along with the yield stress

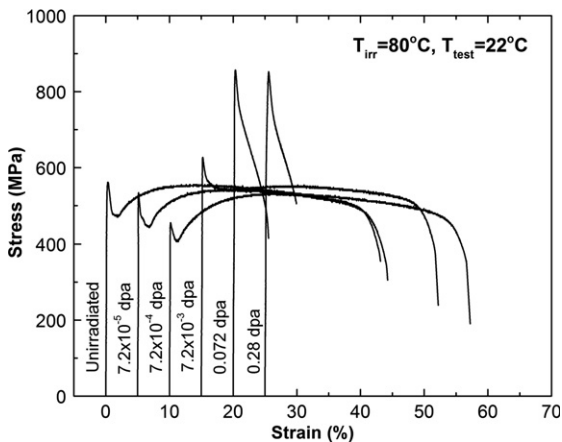


Fig. 4. Stress–strain curves of neutron-irradiated Mo tested at room temperature.

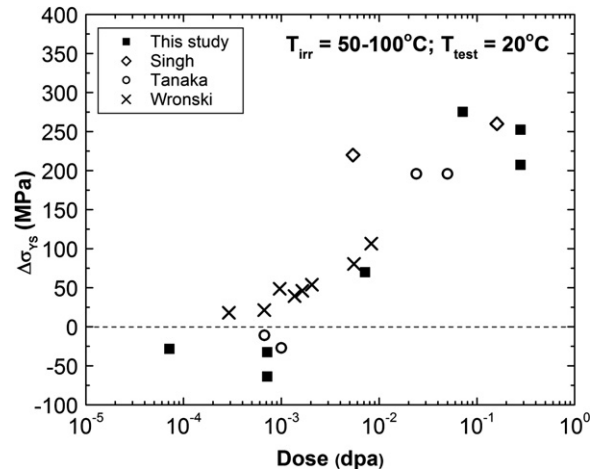


Fig. 5. Dose dependence of the yield stress of neutron-irradiated Mo tested at room temperature.

data of Mo irradiated at 50–100 °C from previous studies [11,12,14]. Irradiation softening was observed at low doses ( $<0.001$  dpa), and irradiation hardening at higher doses. Irradiation softening was also observed in Tanaka et al.'s study [11], but not seen in Wronski et al.'s work [14]. The radiation hardening of Mo increased monotonically with increasing dose from 0.001 dpa up to 0.072 dpa. An apparent hardening saturation was observed between 0.072 and 0.28 dpa when plastic instability occurred at yield, resulting in near zero uniform elongations.

## 4. Discussion

The central focus of this study is to understand the in-cascade point defect clustering behavior and its contribution to sessile defect cluster formation in neutron-irradiated Mo. Whether the sessile defect clusters are produced directly in displacement cascades or formed through homogeneous nucleation and growth can be elucidated by evaluating the dose dependence of number density and mean size of defect clusters. The linear dose accumulation rate and size independence of defect clusters produced in low temperature and low dose irradiations are generally taken as strong evidence of in-cascade defect cluster formation [3,15,16]. In the present study, both the electrical resistivity and the number density of visible defect clusters exhibit a sublinear dose dependence before reaching saturation, as shown in Fig. 6. The saturation effect above 0.1 dpa may be explained by cascade overlap effects

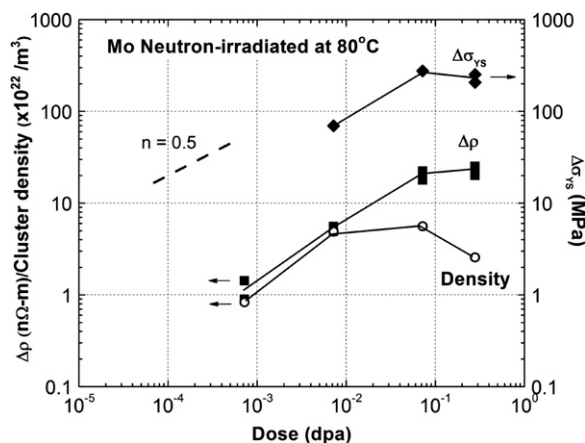


Fig. 6. Dose dependence of defect cluster density, changes in electrical resistivity and changes in the yield stress of neutron-irradiated Mo.

[1,15]. The sublinear defect accumulation behavior in irradiated Mo cannot be explained by in-cascade defect cluster formation. The saturation and reduction in defect number density at moderate and high doses also imply that the formation of sessile defect clusters involves significant nucleation and growth. Furthermore, there is a lack of visible defect clusters at very low doses, where displacement cascades are largely separated and the probability of cluster formation from point defect nucleation and growth is small. MD cascade simulations predicted that a majority of interstitial defect clusters in irradiated Mo were composed of only a few defects and most were glissile [17]. A large number density of interstitial-type defect clusters visible by TEM at high doses are most likely formed by the interactions between small glissile interstitial defects in irradiated Mo. TEM characterization also showed that the mean size of defect clusters increases with increasing dose. The growth of small defect clusters provides further evidence that the visible defect clusters are not produced in displacement cascades in irradiated Mo.

The formation and accumulation mechanisms of defect clusters can be further understood by analyzing the dose dependence of radiation hardening. Neutron irradiation of Mo at 80 °C results in a significant increase in the yield stress only at doses above 0.001 dpa. Significant softening was found at low doses. The lack of substantial hardening at low doses implies that the level of in-cascade clustering is not significant in Mo. When the hardening effect is evaluated by applying TEM measurements of defect density and mean size to the dispersed bar-

rier model [18], the values of defect barrier strength,  $\alpha$  for loops increased with increasing dose, from 0.06 to 0.22–0.27. The increase with dose implies that the sessile defect clusters that cause the hardening effect were not at steady state, but developed during irradiation. It also implies that there may be a population of hardening centers that are not visible by TEM. The increase in electrical resistivity and the decrease in visible cluster density above 0.01 dpa support this hypothesis.

## 5. Conclusions

The major types of defect structure in Mo were loops and rafts in the dose range  $7.2 \times 10^{-4}$  to 0.28 dpa at 80 °C. Defect clusters are not visible at  $7.2 \times 10^{-5}$  dpa. As dose increases both the density and size of defect clusters increased. Raft formation became evident at 0.0072 dpa. Neutron irradiation at low doses decreases the yield strength of Mo. A significant increase in the yield stress occurred above 0.001 dpa accompanied by a decrease in ductility. There is significant experimental evidence that defect cluster formation and accumulation in Mo is associated with the nucleation and growth processes rather than due to large point defect clusters produced in displacement cascades.

## Acknowledgements

The research was sponsored by the Office of Fusion Energy Sciences, the US Department of Energy under contract DE-AC05-00OR22725 with Oak Ridge National Laboratory, managed and operated by UT-Battelle, LLC.

## References

- [1] S.J. Zinkle, B.N. Singh, J. Nucl. Mater. 199 (1993) 173.
- [2] M.L. Jenkins, M.A. Kirk, W.J. Phythian, J. Nucl. Mater. 205 (1993) 16.
- [3] S.J. Zinkle, Y. Matsukawa, J. Nucl. Mater. 329–333 (2004) 88.
- [4] G.T. Meadon, Electrical Resistance of Metals, Plenum, New York, 1965.
- [5] R.C. Rau, F.S. D’Aragona, R.L. Ladd, Philos. Mag. 21 (1970) 441.
- [6] D.M. Maher, B.L. Eyre, Philos. Mag. 23 (1971) 409.
- [7] B.L. Eyre, D.M. Maher, A.F. Bartlett, Philos. Mag. 23 (1971) 439.
- [8] M.E. Downey, B.L. Eyre, Philos. Mag. 11 (1965) 53.
- [9] C.A. English, J. Nucl. Mater. 108&109 (1982) 104.
- [10] J.L. Brimhall, B. Mastel, Radiat. Eff. 3 (1970) 203.

- [11] M. Tanaka, K. Fukaya, K. Shiraishi, *Trans. JIM* 20 (1979) 697.
- [12] B.N. Singh, J.H. Evans, A. Horsewell, P. Toft, G.V. Müller, *J. Nucl. Mater.* 258–263 (1998) 865.
- [13] K. Niebel, M. Wilkens, *Phys. Status Solidi (a)* 24 (1974) 591.
- [14] A.S. Wronski, G.A. Sargent, A.A. Johnson, in: *Flow and Fracture of Metals and Alloys in Nuclear Materials*, 1965, p. 69.
- [15] S.J. Zinkle, B.N. Singh, *J. Nucl. Mater.* 351 (2006) 269.
- [16] M. Victoria, N. Baluc, C. Bailat, Y. Dai, M.I. Lупpo, R. Schaublin, B.N. Singh, *J. Nucl. Mater.* 276 (2000) 114.
- [17] P. Pasianot, M. Alurralde, A. Almazouzi, M. Victoria, *Philos. Mag. A* 82 (2002) 1671.
- [18] A.K. Seeger, in: *Second UN Conference on Peaceful Uses of Atomic Energy*, vol. 6, United Nations, New York, 1958, p. 250.